PHYSICAL REVIEW D VOLUME 56, NUMBER 11 1 DECEMBER 1997

$B \to X_q l^+ l^- (q=d,s)$ and determination of $|V_{td}/V_{ts}|$

C. S. Kim*
Department of Physics, Yonsei University, Seoul 120-749, Korea

T. Morozumi†
Department of Physics, Hiroshima University, 1-3-1 Kagamiyama, Higashi Hiroshima, Japan 739

A. I. Sanda‡
Department of Physics, Nagoya University, Chikusa-ku, Nagoya, Japan 464-01

(Received 12 August 1997)

We propose a new method to extract $|V_{td}/V_{ts}|$ from the ratio of the decay distributions $dR/ds \equiv (d\mathcal{B}/ds) \times [B \to X_d l^+ l^-]/(d\mathcal{B}/ds)[B \to X_s l^+ l^-]$. This ratio depends only on the KM ratio $|V_{td}/V_{ts}|$ with 15% theoretical uncertainties, if dilepton invariant mass-squared s is away from the peaks of the possible resonance states, J/ψ, ψ', etc. We also give a detailed *analytical and numerical* analysis on $(d\mathcal{B}/ds)[B \to X_q l^+ l^-](q=d,s)$ and dR/ds. [S0556-2821(97)07423-7]

PACS number(s): 13.20.He

I. INTRODUCTION

The determination of the elements of the Kobayashi-Maskawa (KM) matrix is one of the most important issues in the quark flavor physics. Moreover, the element V_{td} (or V_{ub}) is especially important to the standard model description of CP violation. If it were zero, there would be no CP violation from the KM matrix elements (i.e., within the standard model), and we have to seek for other sources of CP violation in $K_L \to \pi\pi$. Here we study the ratio V_{td}/V_{ts}. In the standard model with the unitarity of the KM matrix, V_{ts} is approximated by $-V_{cb}$, which is directly measured by semileptonic B decays. There are already several ways to determine V_{td} available in the literature.

$|V_{td}|$ can be indirectly extracted through B_d-$\overline{B_d}$ mixing. However, in B_d-$\overline{B_d}$ mixing the large uncertainty of the hadronic matrix elements prevents us from extracting the element of the KM matrix with good accuracy.

A better extraction of $|V_{td}/V_{ts}|$ can be made if B_s-$\overline{B_s}$ is measured as well, because the ratio $f^2_{B_d} B_{B_d} / f^2_{B_s} B_{B_s}$ can be much better determined.

The determination of $|V_{td}/V_{ts}|$ from the ratios of rates of several hadronic two-body B decays, such as $\Gamma(B^0 \to \overline{K^{*}}^0 K^0)/\Gamma(B^0 \to \phi K^0)$, $\Gamma(B^0 \to \overline{K^{*}}^0 K^{*0})/\Gamma(B^0 \to \phi K^{*0})$, $\Gamma(B^+ \to \overline{K^{*}}^0 K^+)/\Gamma(B^+ \to \phi K^+)$, and $\Gamma(B^+ \to \overline{K^{*}}^0 K^{*+})/\Gamma(B^+ \to \phi K^{*+})$ has been also proposed in Ref. [1].

V_{td} can be determined from $K^+ \to \pi^+ \nu \overline{\nu}$ decay within $\sim$15% theoretical uncertainties with the branching fraction $\mathcal{B} \sim 10^{-10}$ [2].

Why do we discuss yet another method to determine V_{td}? The main reason we are interested in B physics is that this area is very likely to yield information about new physics beyond the standard model. We expect that new physics will influence experimentally measurable quantities in different ways. For example, most of us expect that $\Delta B = 2$ transition is more sensitive to new physics than the decay rates. New physics may couple differently to K mesons compared to B mesons. Therefore, it is essential to determine the KM matrix elements in as many different methods as possible.

In this paper, we propose another method to determine $|V_{td}/V_{ts}|$ precisely from the decay distributions $(d\mathcal{B}/ds) \times [B \to X_s l^+ l^-]$ and $(d\mathcal{B}/ds)[B \to X_d l^+ l^-]$, where s is invariant mass-squared of final lepton pair, $l^+ l^-$. In the decays of $B \to X_q l^+ l^-$ $(q=d,s)$, the short distance (SD) contribution comes from the top quark loop diagrams and the long distance (LD) contribution comes from the decay chains due to intermediate charmonium states. Therefore, the former (SD) amplitude is proportional to $V_{tq}{}^* V_{tb}$, and the latter (LD) proportional to $V_{cq}{}^* V_{cb}$. If the invariant mass-squared of $l^+ l^-$ is away from the peaks of the charmonium resonances (J/ψ and ψ'), the SD contribution is dominant, while on the peaks of the resonances the LD contribution is dominant, and therefore we expect that in the SU(3) symmetry limit the ratio

$$\frac{dR}{ds} \equiv \frac{d\mathcal{B}}{ds}(B \to X_d l^+ l^-) \bigg/ \frac{d\mathcal{B}}{ds}(B \to X_s l^+ l^-)$$

becomes

$$\begin{aligned} \frac{1}{\lambda^2} \frac{dR(s)}{ds} &\to (1-\rho)^2 + \eta^2 \quad (s \to 1 \ \ \mathrm{GeV}^2), \\ &\to 1 \quad (s \to m_{J/\psi}{}^2), \end{aligned} \tag{1}$$

where λ is $\sin\theta_c$, $\theta_c =$ Cabibbo angle, and for ρ, η, see Eq. (8). In the intermediate region, there is a characteristic interference beteen the LD contribution and the SD contribution, which requires the detailed study of the distributions. By

*Electronic address: kim@cskim.yonsei.ac.kr; cskim@kekvax.kek.jp
†Electronic address: morozumi@theo.phy.sci.hiroshima-u.ac.jp
‡Electronic address: sanda@eken.phys.nagoya-u.ac.jp

0556-2821/97/56(11)/7240(7)/$10.00 56 7240

focusing on the region, $1(\mathrm{GeV}^2)\leqslant s<m_{J/\psi}^2$, we can study $|V_{td}/V_{ts}|$ from the experimental ratio of the distributions dR/ds.

We stress the advantages to use the inclusive semileptonic decays.

If dilepton invariant mass-squared s is away from the peaks of the possible intermediate states, J/ψ, ψ', ρ, ω, and etc., the short distance contribution due to top quark loop is dominant. Therefore, we may extract very precisely the combination of $|V_{td}/V_{ts}|$ from the decay distributions within the range $1(\mathrm{GeV}^2)\leqslant s<m_{J/\Psi}{}^2$ without any theoretical uncertainties from the LD hadronic matrices, unknown KM matrix elements, and etc.

Inclusive decay distributions are theoretically well predicted by heavy quark mass expansion away from the phase space boundary. The leading order of the expansion agrees with the parton model result. Furthermore, nonperturbative $1/m_b{}^2$ power corrections of QCD can be easily incorporated.

This paper is organized as follows. In Sec. II, we present the analytic formulas for $(d\mathcal{B}/ds)[B\to X_s l^+ l^-]$ and $(d\mathcal{B}/ds)[B\to X_d l^+ l^-]$. We also show in detail the decay distribution $(d\mathcal{B}/ds)[B\to X_s l^+ l^-]$ including the uncertainties coming from top quark mass m_t and the scale of renormalization group μ. In Sec. III, after brief discussion on the limit of KM elements coming from B_d-$\overline{B_d}$ mixing and $B\to X_u l\overline{\nu}$, we study the ratio of the decay distributions, and show how we may extract $|V_{td}/V_{ts}|$.

II. EFFECTIVE HAMILTONIAN FOR $b\to q l^+ l^-$ AND THEIR DIFFERENTIAL DECAY RATES

In this section, the differential decay rates for $B\to X_q l^+ l^-$ $(q=d,s)$ are shown including both LD and SD effects as well as $\Lambda_{\mathrm{QCD}}^2/m_b{}^2$ power corrections. (See [3] for $b\to d l^+ l^-$, [4] for $b\to s l^+ l^-$, and [5,6] for $B\to X_s l^+ l^-$ including the $1/m_b{}^2$ power corrections.) We also show in detail how the differential decay rate varies by changing the input parameters m_t, and the renormalization scale μ. In Table I, we summarize all the values of the input parameters used in our numerical calculations of decay rates. We use the central values for those input parameters, unless otherwise specified.

The effective Hamiltonian for $b\to q l^+ l^-$ $(q=d,s)$ is given as

$$\mathcal{H}_{\mathrm{eff}}=-\frac{4G_F}{\sqrt{2}}V_{tq}^{*}V_{tb}\left[\sum_{i=1}^{10}C_iO_i\right]+\frac{4G_F}{\sqrt{2}}V_{uq}^{*}V_{ub}[C_1(O_1{}^u-O_1)+C_2(O_2{}^u-O_2)],\tag{2}$$

where V_{ij} are the KM matrix elements. The operators are given as

$$O_1=(\overline{q}_{L\alpha}\gamma_\mu b_{L\alpha})(\overline{c}_{L\beta}\gamma^\mu c_{L\beta}),$$

$$O_2=(\overline{q}_{L\alpha}\gamma_\mu b_{L\beta})(\overline{c}_{L\beta}\gamma^\mu c_{L\alpha}),$$

TABLE I. Values of the input parameters used in the numerical calculations of the decay rates. Unless otherwise specified, we use the central values.

Parameter	Value
m_W	80.26 (GeV)
m_Z	91.19 (GeV)
$\sin^2\theta_W$	0.2325
m_s	0.2 (GeV)
m_d	0.01 (GeV)
m_c	1.4 (GeV)
m_b	4.8 (GeV)
m_t	175 ± 9 (GeV)
μ	$5^{+5.0}_{-2.5}$ (GeV)
$\Lambda_{\mathrm{QCD}}^{(5)}$	$0.214^{+0.066}_{-0.054}$ (GeV)
$\alpha_{\mathrm{QED}}^{-1}$	129
$\alpha_s(m_Z)$	0.117 ± 0.005
$\mathcal{B}_{sl}$	(10.4 ± 0.4) %
λ_1	-0.20 (GeV^2)
λ_2	$+0.12$ (GeV^2)

$$O_3=(\overline{q}_{L\alpha}\gamma_\mu b_{L\alpha})\sum_{q'=u,d,s,c,b}(\overline{q'}_{L\beta}\gamma^\mu q'_{L\beta}),$$

$$O_4=(\overline{q}_{L\alpha}\gamma_\mu b_{L\beta})\sum_{q'=u,d,s,c,b}(\overline{q'}_{L\beta}\gamma^\mu q'_{L\alpha}),$$

$$O_5=(\overline{q}_{L\alpha}\gamma_\mu b_{L\alpha})\sum_{q'=u,d,s,c,b}(\overline{q'}_{R\beta}\gamma^\mu q'_{R\beta}),$$

$$O_6=(\overline{q}_{L\alpha}\gamma_\mu b_{L\beta})\sum_{q'=u,d,s,c,b}(\overline{q'}_{R\beta}\gamma^\mu q'_{R\alpha}),$$

$$O_7=\frac{e}{16\pi^2}\overline{q}_\alpha\sigma_{\mu\nu}(m_bR+m_qL)b_\alpha F^{\mu\nu},$$

$$O_8=\frac{g}{16\pi^2}\overline{q}_\alpha T^a_{\alpha\beta}\sigma_{\mu\nu}(m_bR+m_qL)b_\beta G^{a\mu\nu},$$

$$O_1{}^u=(\overline{q}_{L\alpha}\gamma_\mu b_{L\alpha})(\overline{u}_{L\beta}\gamma^\mu u_{L\beta}),$$

$$O_2{}^u=(\overline{q}_{L\alpha}\gamma_\mu b_{L\beta})(\overline{u}_{L\beta}\gamma^\mu u_{L\alpha}),$$

$$O_9=\frac{e^2}{16\pi^2}\overline{q}_\alpha\gamma^\mu Lb_\alpha\overline{l}\gamma_\mu l,$$

$$O_{10}=\frac{e^2}{16\pi^2}\overline{q}_\alpha\gamma^\mu Lb_\alpha\overline{l}\gamma_\mu\gamma_5 l,\tag{3}$$

where L and R denote chiral projections, $L(R)=1/2(1\mp\gamma_5)$. We use the Wilson coefficients given in the literature (see, for example, [7]).

With the effective Hamiltonian in Eq. (2), the matrix element for the decays $b\to q l^+ l^-$ $(q=d,s)$ can be written as

TABLE II. μ (in GeV) dependence of the Wilson coefficients used in the numerical calculations. The values of $\Lambda_{\rm QCD}$ and m_t are fixed at their central values.

μ	C_1	C_2	C_3	C_4	C_5	C_6	$C_7^{\rm eff}$	$C_9^{\rm NDR}$	$C^{(0)}$
5	−0.2404	1.1031	0.0107	−0.0249	0.0072	−0.0302	−0.3110	4.1530	0.3805
10	−0.1606	1.0642	0.0068	−0.0170	0.0051	−0.0194	−0.2768	3.7551	0.5816
2.5	−0.3472	1.1614	0.0163	−0.0348	0.0096	−0.0462	−0.3525	4.4128	0.1163

$$\mathcal{M}(b\to q l^+l^-)=\frac{G_F\alpha}{\sqrt{2}\pi}V_{tq}^*V_{tb}\Bigg[(C_{9q}^{\rm eff}-C_{10})(\overline{q}\gamma_\mu Lb)\times(\overline{l}\gamma^\mu Ll)+(C_{9q}^{\rm eff}+C_{10})(\overline{q}\gamma_\mu Lb)(\overline{l}\gamma^\mu Rl)-2C_7^{\rm eff}\left(\overline{q}i\sigma_{\mu\nu}\frac{q^\nu}{q^2}(m_qL+m_bR)b\right)(\overline{l}\gamma^\mu l)\Bigg], \tag{4}$$

where $C_{9q}^{\rm eff}$ is given by

$$C_{9q}^{\rm eff}(\hat{s})\equiv C_9\left(1+\frac{\alpha_s(\mu)}{\pi}\omega(\hat{s})\right)+Y_{\rm SD}^q(\hat{s})+Y_{\rm LD}^q(\hat{s}), \tag{5}$$

where q^ν is the four momentum of l^+l^-, $s=q^2$, and $\hat{s}=s/m_b{}^2$. The function $Y_{\rm SD}^q(\hat{s})$ is the one-loop matrix element of O_9, and $Y_{\rm LD}^q(\hat{s})$ is the LD contributions due to the vector mesons mesons J/ψ, ψ', and higher resonances. The function $\omega(\hat{s})$ represents the $O(\alpha_s)$ correction from the one-gluon exchange in the matrix element of O_9, and is given in our Appendix. The two functions $Y_{\rm SD}^q$ and $Y_{\rm LD}^q$ are written as

$$\begin{aligned}Y_{\rm SD}^q(\hat{s})=&\,g(\hat{m}_c,\hat{s})(3C_1+C_2+3C_3+C_4+3C_5+C_6)\\&-\frac{1}{2}g(1,\hat{s})(4C_3+4C_4+3C_5+C_6)\\&-\frac{1}{2}g(0,\hat{s})(C_3+3C_4)+\frac{2}{9}(3C_3+C_4+3C_5+C_6)\\&-\frac{V_{uq}^*V_{ub}}{V_{tq}^*V_{tb}}(3C_1+C_2)[g(0,\hat{s})-g(\hat{m}_c,\hat{s})],\end{aligned} \tag{6}$$

$$\begin{aligned}Y_{\rm LD}^q(\hat{s})=&\,\frac{3}{\alpha^2}\kappa\left(-\frac{V_{cq}^*V_{cb}}{V_{tq}^*V_{tb}}C^{(0)}-\frac{V_{uq}^*V_{ub}}{V_{tq}^*V_{tb}}(3C_3+C_4+3C_5+C_6)\right)\\&\times\sum_{V_i=\psi(1s),\ldots,\psi(6s)}\frac{\pi\Gamma(V_i\to l^+l^-)M_{V_i}}{M_{V_i}{}^2-\hat{s}m_b{}^2-iM_{V_i}\Gamma_{V_i}},\end{aligned} \tag{7}$$

where the function $g(\hat{m}_c=m_c/m_b,\hat{s})$, $g(1,\hat{s})$, and $g(0,\hat{s})$ represent c quark, b quark, and u,d,s quark loop contributions, respectively. The two functions $g(z,\hat{s})$ and $g(0,\hat{s})$ are given [7] in our Appendix. In Eq. (7), $C^{(0)}\equiv 3C_1+C_2+3C_3+C_4+3C_5+C_6$, and the first two terms are dominant, as can be seen from Table II.

It is convenient to write the relevant combinations of KM in terms of the Wolfenstein parametrization. In the following, in addition to A and λ, we choose $(1-\rho)^2+\eta^2$ and $\phi_1=\arg(-V_{cd}V_{cb}^*/V_{td}V_{tb}^*)$ as independent variables, then we have

$$\begin{aligned}V_{ts}^*V_{tb}&\simeq\lambda^2A,\\ \frac{V_{cs}^*V_{cb}}{V_{ts}^*V_{tb}}&\simeq-1,\\ \frac{V_{us}^*V_{ub}}{V_{ts}^*V_{tb}}&=O(\lambda^2),\\ V_{td}^*V_{tb}&\simeq\lambda^3A(1-\rho+i\eta),\\ \frac{V_{cd}^*V_{cb}}{V_{td}^*V_{tb}}&\simeq-\frac{1}{1-\rho+i\eta},\\ &=-\frac{\exp(-i\phi_1)}{\sqrt{(1-\rho)^2+\eta^2}},\\ \frac{V_{ud}^*V_{ub}}{V_{td}^*V_{tb}}&\simeq\frac{\rho-i\eta}{1-\rho+i\eta},\\ &=-1+\frac{\exp(-i\phi_1)}{\sqrt{(1-\rho)^2+\eta^2}}.\end{aligned} \tag{8}$$

In the SD contribution of $B\to X_sl^+l^-$, the u-quark loop contribution is neglected due to the smallness of the combination $V_{us}^*V_{ub}$ compared with $V_{cs}^*V_{cb}\simeq-V_{ts}^*V_{tb}$, while in $B\to X_dl^+l^-$ the term which is proportional to $V_{ud}^*V_{ub}$ is maintained. In the LD contribution, there is a contribution coming from the gluonic penguin amplitude which is proportional to $(V_{ud}^*V_{ub}/V_{td}^*V_{tb})(3C_3+C_4+3C_5+C_6)$. This contribution is neglected because of the smallness of the Wilson coefficient $(3C_3+C_4+3C_5+C_6)$ compared with $C^{(0)}$. We adopt $\kappa=2.3$ [8] to reproduce the rate of the decay chain $B\to X_sJ/\psi\to X_sl^+l^-$. Note that the data determine only the combination, $\kappa C^{(0)}=0.88$.

By combining both SD and LD contributions as well as nonperturbative $1/m_b{}^2$ power corrections, the differential decay rate for $B\to X_ql^+l^-$ $(q=d,s)$ becomes

TABLE III. $\Lambda_{\rm QCD}{}^5$ dependence of the Wilson coefficients used in the numerical calculations. The values of m_t and μ are fixed at their central values.

$\Lambda_{\rm QCD}{}^5$	C_1	C_2	C_3	C_4	C_5	C_6	$C_7^{\rm eff}$	$C_9^{\rm NDR}$	$C^{(0)}$
0.214	−0.2404	1.1031	0.0107	−0.0249	0.0072	−0.0302	−0.3110	4.1530	0.3805
0.280	−0.2579	1.1122	0.0116	−0.0265	0.0076	−0.0327	−0.3181	4.2137	0.3369
0.160	−0.2242	1.0949	0.0099	−0.0233	0.0068	−0.0279	−0.3043	4.0891	0.4212

$$
\begin{aligned}
\frac{d\mathcal{B}}{d\hat{s}} = {} & 2\frac{|V_{tq}^{*}V_{tb}|^2}{|V_{cb}|^2}\mathcal{B}_0\Bigg\{\Bigg(\frac{2}{3}\hat{u}(\hat{s},\hat{m}_q)[(1-\hat{m}_q^2)^2+\hat{s}(1+\hat{m}_q^2)-2\hat{s}^2]+\frac{1}{3}(1-4\hat{m}_q^2+6\hat{m}_q^4-4\hat{m}_q^6+\hat{m}_q^8-\hat{s}+\hat{m}_q^2\hat{s}+\hat{m}_q^4\hat{s}-\hat{m}_q^6\hat{s}-3\hat{s}^2 \\
& -2\hat{m}_q^2\hat{s}^2-3\hat{m}_q^4\hat{s}^2+5\hat{s}^3+5\hat{m}_q^2\hat{s}^3-2\hat{s}^4)\frac{\hat{\lambda}_1}{\hat{u}(\hat{s},\hat{m}_q)}+(1-8\hat{m}_q^2+18\hat{m}_q^4-16\hat{m}_q^6+5\hat{m}_q^8-\hat{s}-3\hat{m}_q^2\hat{s}+9\hat{m}_q^4\hat{s}-5\hat{m}_q^6\hat{s}-15\hat{s}^2 \\
& -18\hat{m}_q^2\hat{s}^2-15\hat{m}_q^4\hat{s}^2+25\hat{s}^3+25\hat{m}_q^2\hat{s}^3-10\hat{s}^4)\frac{\hat{\lambda}_2}{\hat{u}(\hat{s},\hat{m}_q)}\Bigg)(|C_9^{\rm eff}|^2+|C_{10}|^2)+\Bigg(\frac{8}{3}\hat{u}(\hat{s},\hat{m}_q)[2(1+\hat{m}_q^2)(1-\hat{m}_q^2)^2 \\
& -(1+14\hat{m}_q^2+\hat{m}_q^4)\hat{s}-(1+\hat{m}_q^2)\hat{s}^2]+\frac{4}{3}(2-6\hat{m}_q^2+4\hat{m}_q^4+4\hat{m}_q^6-6\hat{m}_q^8+2\hat{m}_q^{10}-5\hat{s}-12\hat{m}_q^2\hat{s}+34\hat{m}_q^4\hat{s}-12\hat{m}_q^6\hat{s}-5\hat{m}_q^8\hat{s} \\
& +3\hat{s}^2+29\hat{m}_q^2\hat{s}^2+29\hat{m}_q^4\hat{s}^2+3\hat{m}_q^6\hat{s}^2+\hat{s}^3-10\hat{m}_q^2\hat{s}^3+\hat{m}_q^4\hat{s}^3-\hat{s}^4-\hat{m}_q^2\hat{s}^4)\frac{\hat{\lambda}_1}{\hat{u}(\hat{s},\hat{m}_q)}+4(-6+2\hat{m}_q^2+20\hat{m}_q^4-12\hat{m}_q^6-14\hat{m}_q^8 \\
& +10\hat{m}_q^{10}+3\hat{s}+16\hat{m}_q^2\hat{s}+62\hat{m}_q^4\hat{s}-56\hat{m}_q^6\hat{s}-25\hat{m}_q^8\hat{s}+3\hat{s}^2+73\hat{m}_q^2\hat{s}^2+101\hat{m}_q^4\hat{s}^2+15\hat{m}_q^6\hat{s}^2+5\hat{s}^3-26\hat{m}_q^2\hat{s}^3+5\hat{m}_q^4\hat{s}^3-5\hat{s}^4 \\
& -5\hat{m}_q^2\hat{s}^4)\frac{\hat{\lambda}_2}{\hat{u}(\hat{s},\hat{m}_q)}\Bigg)\frac{|C_7^{\rm eff}|^2}{\hat{s}}+\Bigg[8\hat{u}(\hat{s},\hat{m}_q)[(1-\hat{m}_q^2)^2-(1+\hat{m}_q^2)\hat{s}]+4(1-2\hat{m}_q^2+\hat{m}_q^4-\hat{s}-\hat{m}_q^2\hat{s})\hat{u}(\hat{s},\hat{m}_q)\hat{\lambda}_1+4(-5 \\
& +30\hat{m}_q^4-40\hat{m}_q^6+15\hat{m}_q^8-\hat{s}+21\hat{m}_q^2\hat{s}+25\hat{m}_q^4\hat{s}-45\hat{m}_q^6\hat{s}+13\hat{s}^2+22\hat{m}_q^2\hat{s}^2+45\hat{m}_q^4\hat{s}^2-7\hat{s}^3-15\hat{m}_q^2\hat{s}^3) \\
& \times\frac{\hat{\lambda}_2}{\hat{u}(\hat{s},\hat{m}_q)}\Bigg]{\rm Re}(C_9^{\rm eff})C_7^{\rm eff}\Bigg\}. \qquad (9)
\end{aligned}
$$

We explain some aspect of the expression (9).

The branching ratio is normalized by $\mathcal{B}_{sl}$ of decays $B\to(X_c,X_u)l\nu_l$. We separate a combination of the KM factor $|V_{tq}^{*}V_{tb}|^2/|V_{cb}|^2$ due to top-quark loop from the normalization factor $\mathcal{B}_0$. The normalization constant $\mathcal{B}_0$ is

$$
\mathcal{B}_0 \equiv \mathcal{B}_{sl}\frac{3\alpha^2}{16\pi^2}\frac{1}{f(\hat{m}_c)\kappa(\hat{m}_c)}, \qquad (10)
$$

where $f(\hat{m}_c)$ is a phase space factor, and $\kappa(\hat{m}_c)$ accounts for both the $O(\alpha_s)$ QCD correction to the semileptonic decay width and the leading order $(1/m_b)^2$ power correction. They are given in our Appendix explicitly.

The Wilson coefficients depend on the top quark mass m_t, the renormalization scale μ, and $\Lambda_{\rm QCD}$. Their dependences are studied in Tables II, III, and IV. As the value of μ ($\Lambda_{\rm QCD}$) decreases (increases), $|C_7|$ and C_9 are getting larger, while C_{10} is independent on μ. As m_t increases, $|C_7|$, C_9, and $|C_{10}|$ all become larger. The matrix elements also depend on the renormalization scale μ, and their dependence is partially canceled by the given dependence of the Wilson coefficients. The overall dependence can be studied with the differential rate. In Figs. 1 and 2, we show the dependence of the differential rate on m_t and μ. As the value of m_t increases from 166 (GeV) to 184 (GeV), the differential rate increases about 20% at $s\sim5$ (GeV^2), as shown in Fig. 1. At around the same region of s, by changing μ from 2.5 (GeV) to 10 (GeV) the differential rate increases about 20%, as shown in Fig. 2. This observation is consistent with the result of Ref. [7], in which only the SD contribution has been analyzed.

The differential decay rate (9) is not a simple parton model result. It contains nonperturbative $1/m_b{}^2$ power cor-

TABLE IV. m_t dependence of the Wilson coefficients used in the numerical calculations. The values of $\Lambda_{\rm QCD}{}^5$ and μ are fixed at their central values.

m_t	$C_7^{\rm eff}$	$C_9^{\rm NDR}$	C_{10}
175	−0.311	4.153	−4.546
166	−0.3066	4.0796	−4.1877
184	−0.3150	4.2238	−4.9156

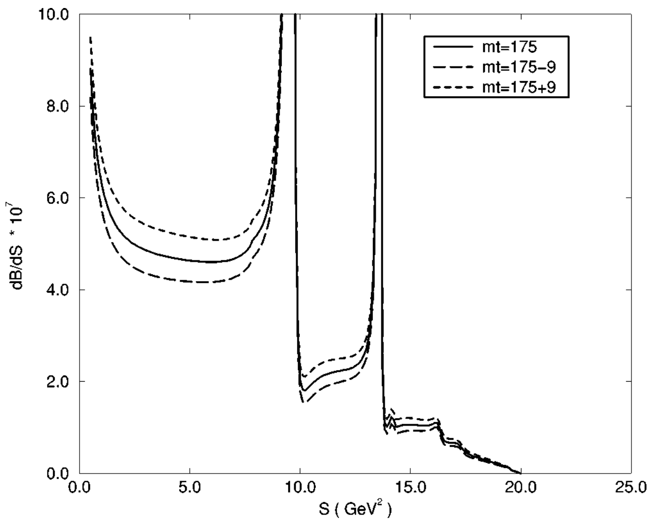

FIG. 1. Dilepton invariant mass spectrum, $(d\mathcal{B}/ds) \times(B \rightarrow X_s e^+ e^-)\times 10^7$. The unit of s is (GeV^2). The solid line corresponds to $m_t=175$ (GeV). The short-dashed line corresponds to $m_t=175+9$. The long-dashed line corresponds to $m_t=175-9$.

rections, which are denoted in Eq. (9) by the terms proportional to $\hat{\lambda}_1$ and $\hat{\lambda}_2$. The parameters $\hat{\lambda}_1$ and $\hat{\lambda}_2$ are related to the matrix elements of the higher derivative operators of heavy quark effective theory [5,9];

$$\langle B|\overline{h}(iD)^2 h|B\rangle \equiv 2M_B\lambda_1 = 2M_B {m_b}^2\hat{\lambda}_1,$$

$$\left\langle B\left|\overline{h}\frac{-i}{2}\sigma^{\mu\nu}G_{\mu\nu}h\right|B\right\rangle \equiv 6M_B\lambda_2 = 6M_B {m_b}^2\hat{\lambda}_2, \quad (11)$$

where B denotes the pseudoscalar B meson, D_μ is the covariant derivative, and $G_{\mu\nu}$ is the QCD field strength tensor.

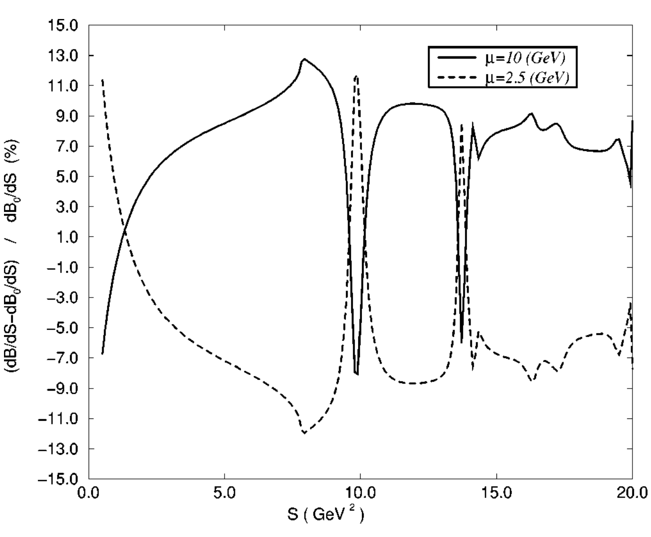

FIG. 2. The % variation of dilepton invariant mass spectrum defined as $(d\mathcal{B}(\mu)/ds - d\mathcal{B}_0/ds)/(d\mathcal{B}_0/ds)$; $\mathcal{B}_0=\mathcal{B}[\mu=5\ (\mathrm{GeV})]$. The solid line corresponds to $\mu=10$ and the dashed line corresponds to $\mu=2.5$.

III. THE EXTRACTION OF $|V_{td}/V_{ts}|$

Presently we can constrain the value of $(1-\rho)^2+\eta^2$ from $B_d-\overline{B_d}$ mixing, while from $B\rightarrow X_u l \overline{\nu}$ we obtain some limit on $\rho^2+\eta^2$. Using those given limits, we can show how the ratio $(1/\lambda^2)(dR/ds)$ depends on input KM values, $(1-\rho)^2+\eta^2$ and ϕ_1 (or β).

As is well known, $|V_{tb}^* V_{td}|$ are written with ΔM_d of B_d-$\overline{B_d}$ mixing. It reads

$$|V_{tb}^* V_{td}| = A\lambda^3\sqrt{(1-\rho)^2+\eta^2} = \left[\frac{6\pi^2}{G_F^2\eta_{\mathrm{QCD}}M_W^2 M_B}\right]^{1/2}\left[\frac{\Delta {M_d}^{1/2}}{B_{B_d}^{1/2} f_{B_d}|E(x_t)|^{1/2}}\right], \quad (12)$$

where $E(x_t)$ is the Inami-Lim function [10] of the box diagram, and $x_t \equiv {m_t}^2/{m_W}^2$. It has the value $|E(x_t)|=2.58$ for $m_t=175$ (GeV) and it varies from 2.38 to 2.78 as m_t varies from 166 (GeV) to 184 (GeV). We use the following values: $\eta_{\mathrm{QCD}}=0.55$, $m_t=175$ (GeV), and the experimental constraints

$$\Delta M_d = 0.474 \pm 0.031\ (\mathrm{ps}^{-1}),$$

$$|V_{ub}/V_{cb}| = \lambda\sqrt{\rho^2+\eta^2} = 0.08 \pm 0.02. \quad (13)$$

Then, those constraints (13) are translated into the limits of $(1-\rho)^2+\eta^2$ and $\sqrt{\rho^2+\eta^2}$ as

$$(1-\rho)^2+\eta^2 = 0.85(1\pm 0.15)\{0.2/[B_{B_d}^{1/2} f_{B_d}(\mathrm{GeV})]\}^2 = (0.59\pm 0.09, 1.3\pm 0.20),$$

$$\sqrt{\rho^2+\eta^2} = 0.36\pm 0.09. \quad (14)$$

Here we used $B_{B_d}^{1/2} f_{B_d} = 0.2 \pm 0.04$ (GeV) to get the range of $(1-\rho)^2+\eta^2 \approx (0.5,1.5)$. We also used $A\lambda^2 = 0.041(\pm 0.003)$, and $\lambda=0.2205$. In Fig. 3, we show the present limit in the plane of $(\phi_1,(1-\rho)^2+\eta^2)$. The horizontal axis corresponds to ϕ_1 (or β), and the unit is degree. The vertical axis corresponds to $(1-\rho)^2+\eta^2$. The thin dashed line is obtained from the central values of $|V_{ub}|$ and the thin solid line is obtained from $|V_{td}|$. The central value corresponds to $(\phi_1,(1-\rho)^2+\eta^2) \approx (20°, 0.85)$.

Now let us consider the ratio $(1/\lambda^2)(dR(s)/ds)$. In the SU(3) limit, we expect that this ratio approaches to the input value of $(1-\rho)^2+\eta^2$ for the dileptonic invariant mass-squared s far below the peak of charmonium resonances. If s is on the peak of resonances, the ratio becomes 1. In Fig. 4, we show the ratio $(1/\lambda^2)(dR(s)/ds)$ for two sets of the assumed input values of $(\phi_1,(1-\rho)^2+\eta^2)$, one of whose $(1-\rho)^2+\eta^2$ is 0.59, and the other is 1.33. They correspond to their small (or large) values allowed from the present experimental result of B_d-$\overline{B_d}$ mixing. The solid curve corresponds to $(\phi_1,(1-\rho)^2+\eta^2)=(20°,0.59)$, and the dot-dashed curve corresponds to (20°,1.33). The ratios for the CP conjugate process $\overline{B}\rightarrow \overline{X_q} l^+ l^-$ are also shown, denoted by the long-dashed curve for $(1-\rho)^2+\eta^2=1.33$, and by the dashed curve for $(1-\rho)^2+\eta^2=0.59$. They are obtained by

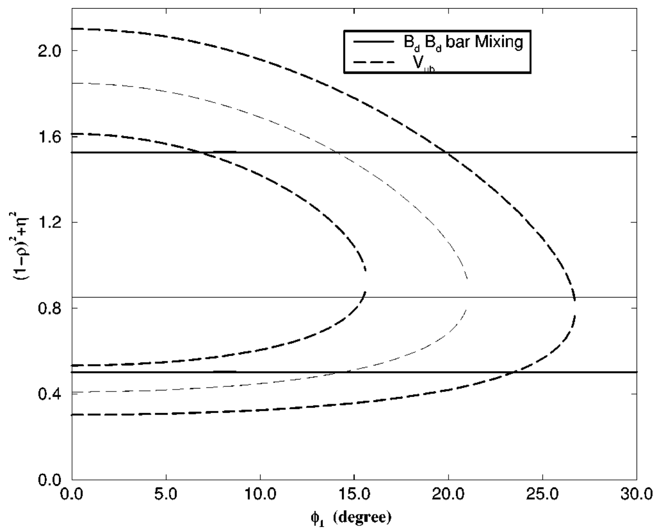

FIG. 3. The limit on $(1-\rho)^2+\eta^2$ and ϕ_1 (or β). The horizontal axis corresponds to ϕ_1, and the unit is degree. The vertical axis corresponds to $(1-\rho)^2+\eta^2$. The thin dashed line and the thin solid line are obtained from the central values of $|V_{ub}|$ and $|V_{td}|$, respectively. The thick solid lines are obtained from the allowed range of $|V_{td}|$ from $B_d\overline{B_d}$ mixing. The thick dashed lines are obtained from the allowed range of $|V_{ub}|$.

reversing the sign of ϕ_1 in the corresponding $B \to X_q l^+ l^-$ process; i.e., $\phi_1 \to -\phi_1$. They are labeled as $(-20°,1.33)$ and $(-20°,0.59)$ in Fig. 4.

To summarize the numerical results of Fig. 4 and Sec. III.

The predicted ratio at low invariant mass region $s \simeq 1$ (GeV^2) is very near to our assumed input value of $(1-\rho)^2+\eta^2$, while on the peak of the resonances J/ψ, ψ', this ratio becomes almost 1, as we expected: i.e.,

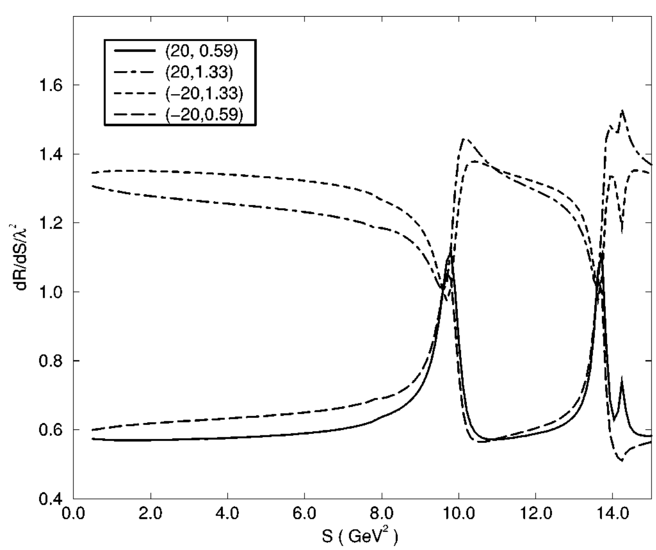

FIG. 4. The ratio $(1/\lambda^2)(dR/ds)$ versus s (GeV^2) with two different input values of $(1-\rho)^2+\eta^2$. The solid curve correspond to $(\phi_1,(1-\rho)^2+\eta^2)=(20°,0.59)$, and the dot-dashed curve corresponds to (20°,1.33). The ratios for CP conjugate process $\overline{B} \to \overline{X_q} l^+ l^-$ are denoted by the dashed curve for $(1-\rho)^2+\eta^2=1.33$, and by the long-dashed curve for $(1-\rho)^2+\eta^2=0.59$. They are obtained by reversing the sign of ϕ_1 in the corresponding $B \to X_q l^+ l^-$ process; i.e., $\phi_1 \to -\phi_1$.

$$(1/\lambda^2)(dR(s)/ds) \to 1 \quad (s \sim m_{J/\psi}{}^2, m_{\psi'}{}^2, \ldots),$$

$$\to (1-\rho)^2+\eta^2$$

$$(s \text{ being away from } m_{J/\psi}{}^2, \ldots). \quad (15)$$

In the intermediate region, there is a characteristic interference between the LD contribution and the SD contribution, which can be only derived from the detailed expression of the distributions, Eq. (9).

The value of the ratio does not depend much on whether the decaying particles are B or $\overline{B}$ at any invariant mass-squared region.

This ratio changes only a few % when we change the input parameters, m_t and μ, within the range shown in Table I. The dependences on m_t and μ are almost canceled away in the ratio. Therefore, the uncertainties in this ratio due to the input parameters are much smaller than the uncertainties in the differential decay rate itself, as shown in Tables II, III, and IV as well as in Figs. 1 and 2.

In Fig. 4 the range between the dot-dashed curve and the solid curve corresponds to the value of the ratio $(1/\lambda^2)(dR(s)/ds)$ allowed from the present experimental result of B_d-$\overline{B_d}$ mixing. Future experimental measurements on the ratio of the branching fractions, $\mathcal{B}(B \to X_d l^+ l^-)$ and $\mathcal{B}(B \to X_s l^+ l^-)$, can give much better alternative for determination of $|V_{td}/V_{ts}|$ without any hadronic uncertainties, limited only by experimental statistics.

If 10^9 $B\overline{B}$ pairs are produced, the expected number of the events for $B \to X_d l^+ l^-$ in the range of $4m_\mu{}^2 < s < 6$ GeV^2 ($m_\mu =$ muon mass) is about 100 for $(1-\rho)^2+\eta^2=0.59$, and is about 220 for $(1-\rho)^2+\eta^2=1.33$. Therefore, the statistical accuracy of $(1-\rho)^2+\eta^2$ determined from this method is about 7%~10% with the expected production of 10^9 $B\overline{B}$ pairs.

We have assumed in our numerical analysis the flavor SU(3) symmetry with $m_d = m_s$. We estimated the corrections due to SU(3) breaking by varying m_d from 0.01 GeV up to $m_s = 0.2$ GeV. And we find the ratio dR/ds decreases within 0.2–0.3% for the range $1 < s < 9$ (GeV^2). Therefore, we conclude the SU(3) breaking effect does not affect the extraction of $|V_{td}/V_{ts}|$ at all.

ACKNOWLEDGMENTS

T.M. would like to thank G. Hiller, K. Ochi, T. Nasuno, and Y. Kiyo for correspondence and assistance in numerical computations. The work of C.S.K. was supported in part by the CTP, Seoul National University, in part by the BSRI Program, Ministry of Education, Project No. BSRI-97-2425, and in part by the KOSEF-DFG large collaboration project, Project No. 96-0702-01-01-2. The work of T.M. was partially supported by Monbusho International Scientific Research Program (No. 08044089), and that of A.I.S. and T.M. was supported also by Grant-in-Aid for Scientific Research on Priorty Areas (Physics of CP violation) from the Ministry of Education and Culture of Japan.

APPENDIX A: FUNCTIONS $G(Z,\hat{s})$, $G(0,\hat{s})$, AND $\omega(\hat{s})$

The functions $g(z,\hat{s})$ and $g(0,\hat{s})$ are given as

$$g(z,\hat{s})=-\frac{8}{9}\ln\left(\frac{m_b}{\mu}\right)-\frac{8}{9}\ln z+\frac{8}{27}+\frac{4}{9}y$$
$$-\frac{2}{9}(2+y)\sqrt{|1-y|}\left[\Theta(1-y)\left(\ln\frac{1+\sqrt{1-y}}{1-\sqrt{1-y}}-i\pi\right)\right.$$
$$\left.+\Theta(y-1)2\arctan\frac{1}{\sqrt{y-1}}\right], \tag{A1}$$

with $y=4z^2/\hat{s}$, and

$$g(0,\hat{s})=\frac{8}{27}-\frac{8}{9}\ln\left(\frac{m_b}{\mu}\right)-\frac{4}{9}\ln\hat{s}+\frac{4}{9}i\pi. \tag{A2}$$

The function $\omega(\hat{s})$ represents the $O(\alpha_s)$ correction from the one-gluon exchange in the matrix element of O_9 [11]:

$$\omega(\hat{s})=-\frac{2}{9}\pi^2-\frac{4}{3}\mathrm{Li}_2(\hat{s})-\frac{2}{3}\ln\hat{s}\ln(1-\hat{s})$$
$$-\frac{5+4\hat{s}}{3(1+2\hat{s})}\ln(1-\hat{s})-\frac{2\hat{s}(1+\hat{s})(1-2\hat{s})}{3(1-\hat{s})^2(1+2\hat{s})}\ln\hat{s}$$
$$+\frac{5+9\hat{s}-6\hat{s}^2}{6(1-\hat{s})(1+2\hat{s})}. \tag{A3}$$

APPENDIX B: FUNCTIONS $F(\hat{m}_C)$ AND $\kappa(\hat{m}_C)$

The phase space function for $\Gamma(B\to X_c l\nu)$ to the lowest order (i.e., parton model) is

$$f(\hat{m}_c)=1-8\hat{m}_c^2+8\hat{m}_c^6-\hat{m}_c^8-24\hat{m}_c^4\ln\hat{m}_c. \tag{B1}$$

And $\kappa(\hat{m}_c)$ accounts for both the $O(\alpha_s)$ QCD correction to the semileptonic decay width and the leading order $(1/m_b)^2$ power correction:

$$\kappa(\hat{m}_c)=1-\frac{2\alpha_s(m_b)}{3\pi}g(\hat{m}_c)+\frac{h(\hat{m}_c)}{2m_b^2}. \tag{B2}$$

The function $g(\hat{m}_c)$ is given [11,12] as

$$g(\hat{m}_c)=\left(\pi^2-\frac{31}{4}\right)(1-\hat{m}_c)^2+\frac{3}{2}, \tag{B3}$$

and finally the function $h(\hat{m}_c)$ is given [9] as

$$h(\hat{m}_c)=\lambda_1+\frac{\lambda_2}{f(\hat{m}_c)}(-9+24\hat{m}_c^2-72\hat{m}_c^4+72\hat{m}_c^6-15\hat{m}_c^8$$
$$-72\hat{m}_c^4\ln\hat{m}_c), \tag{B4}$$

where λ_1 (or $-\mu_\pi^2$) and λ_2 (or μ_G^2) denote the matrix element of the higher derivative operators of heavy quark effective theory, as defined in Eq. (11).

[1] M. Gronau and J.L. Rosner, Phys. Lett. B **376**, 205 (1996).
[2] G. Buchalla and A.J. Buras, Phys. Rev. D **54**, 6782 (1996).
[3] F. Krüger and L.M. Sehgal, Phys. Rev. D **55**, 2799 (1997).
[4] C.S. Lim, T. Morozumi, and A.I. Sanda, Phys. Lett. B **218**, 343 (1989); N.G. Deshpande, J. Trampetic, and K. Panose, Phys. Rev. D **39**, 1461 (1989); P.J. O'Donnell and H.K.K. Tung, *ibid.* **43**, R2067 (1991); A. Ali, T. Mannel, and T. Morozumi, Phys. Lett. B **273**, 505 (1991); N. Paver and Riazuddin, Phys. Rev. D **45**, 978 (1992).
[5] A. Falk, M. Luke, and M.J. Savage, Phys. Rev. D **49**, 3367 (1994).
[6] A. Ali, G. Hiller, L. Handoko, and T. Morozumi, Phys. Rev. D **55**, 4105 (1997).
[7] A.J. Buras and M. Münz, Phys. Rev. D **52**, 186 (1995), and references therein.
[8] Z. Ligeti and M.B. Wise, Phys. Rev. D **53**, 4937 (1996).
[9] I.I. Bigi, M.A. Shifman, N.G. Uraltsev, and A. I. Vainshtein, Phys. Rev. Lett. **71**, 496 (1993); A.V. Manohar and M.B. Wise, Phys. Rev. D **49**, 1310 (1994); B. Blok, L. Koyrakh, M. Shifman, and A.I. Vainshtein, *ibid.* **49**, 335 (1994); T. Mannel, Nucl. Phys. **B423**, 396 (1994); M. Neubert, Phys. Rev. D **49**, 3392 (1994).
[10] T. Inami and C.S. Lim, Prog. Theor. Phys. **65**, 297 (1981); **65**, 1772(E) (1981).
[11] M. Jeżabek and J. H. Kühn, Nucl. Phys. **B320**, 20 (1989).
[12] C.S. Kim and A.D. Martin, Phys. Lett. B **225**, 186 (1989); A. Ali and E. Pietarinen, Nucl. Phys. **B154**, 519 (1979); N. Cabibbo, G. Corbò, and L. Maiani, *ibid.* **B155**, 93 (1979).